SMGroup

SM Journal of Clinical and Medical Imaging

Research Article

Developing a Texture Analysis Technique using Fluid-Attenuated Inversion Recovery (FLAIR) to Differentiate Tumor from Edema for Contouring Primary Intracranial Tumors

Edward Florez[1], Todd A Nichols[1], Seth T Lirette[2], Candace M Howard[1] and Ali Fatemi[1,3]*

[1]*Department of Radiology, University of Mississippi Medical Center, Jackson, USA*
[2]*Department of Data Science, University of Mississippi Medical Center, Jackson, USA*
[3]*Department of Radiation Oncology, University of Mississippi Medical Center, Jackson, USA*

Article Information

Received date: May 12, 2018
Accepted date: May 30, 2018
Published date: Jun 01, 2018

***Corresponding author**

Ali Fatemi, Departments of Radiology and Radiation Oncology, University of Mississippi Medical Center, 2500 North State Street, Jackson, Mississippi 39216, USA, Tel: +1 (601)-815-1778, Fax: +1 (601)-815-0444; Email: afatemi@umc.edu

Keywords Medical Imaging; Radiomics; Texture Analysis; FLAIR; MRI guided radiotherapy; Tumor Delineation; Contouring primary tumor

Abbreviations ADC: Apparent Diffusion Coefficients; AUC: Area Under The Curve; CT: Computed Tomography; FOS: First-Order Statistics; FLAIR: Fluid-Attenuated Inversion Recovery; GBM: Glioblastoma Multiforme; GLCM: Grey Level Co-Occurrence Matrix; GLRLM: Grey-Level Run Length Matrix; HOS: Higher-Order Statistics; IRB: Institutional Review Board; LASSO: Least Absolute Shrinkage And Selection Operator; LDA: Linear Discriminant Analysis; MRI: Magnetic Resonance Imaging; PCA: Principal Components Analysis; ROC: Receiver Operating Characteristic; ROI: Regions Of Interest; SD: Standard Deviation; SOS: Second-Order Statistics; TE: Echo Time; TI: Inversion Time; TR: Repetition Time; T2W: T2 weighted; WHO: World Health Organization

Abstract

Purpose: Treatment protocols for malignant tumors generally call for surgical removal followed by tumor-bed irradiation. Irradiation ideally affects the tumor volume while limiting damage to surrounding normal tissues; this requires accurate determination of 3-D treatment volumes. Glioblastoma multiforme (GBM) and meningioma are common primary intracranial tumors. Edema surrounding meningioma is vasogenic, while edema surrounding GBM may also have tumor cell infiltration, difficult to differentiate by Fluid-Attenuated Inversion Recovery (FLAIR). Hypothetically, the FLAIR signals of edema and GBM should differ. We used T2W-FLAIR spin-echo to determine edema type and differentiate tumors through their textural properties.

Methods: Enrollment was 20 patients with GBM and 10 with meningioma. Patients were scanned using a 3-D multiecho GRE sequence, measuring the FLAIR signal of edema around the tumor. Segmentation identified two regions of interest (ROI, edema and tumor); texture analysis was applied to each ROI with- and without normalization. LASSO analysis of texture parameters selected the best parameters for separating ROIs; using them, we performed a Receiver Operating Characteristic (ROC) analysis.

Results: Two intracranial tumor types with- and without normalization provided four scenarios per ROI. First-order statistics using 1%-percentile feature was chosen in all scenarios and had the best discriminant ability for meningioma. Second-order statistics using correlation features was also selected across scenarios, although angle and magnitude varied. Higher-order statistics using short-run emphasis features and gray level non-uniformity provided the best discrimination for GBM images with- and without normalization, respectively. ROC curves display the results of both the single best discriminator and the discriminant ability of the model using all features selected by LASSO. All univariate models had good discriminant ability (AUC>0.83), and all multivariate models had excellent discriminant ability (AUC>0.92).

Conclusion: A small subset of texture parameters shows excellent ability to discriminate edema from tumor tissue through its most discriminating features.

Introduction

Tumor volume is a significant prognostic factor in the treatment of malignant tumors. Treatment protocols for malignant brain tumors generally call for removal through surgical procedures followed by irradiation of the tumor bed. The goal of radiation therapy is to irradiate the tumor volume while limiting damage to the surrounding normal tissues. Achieving this goal requires accurate determination of 3-D treatment volumes.

Tumor volume is a significant prognostic factor in the treatment of malignant tumors [1]. Even though CT is the standard procedure applied in patients with intracranial tumors due to its high acquisition speed, low cost, and low sensitivity to patient motion during examination, this modality has clear limitations due to its use of ionizing radiation and the limited reduced range of soft tissue contrast in the resulting images. The reduced soft tissue contrast within CT images may affect the identification of lesions in the brain and means such images are not appropriate to use for definitive diagnosis. Contemporaneously, the capabilities of the MRI modality have been gaining prominence, being able to obtain images with superior quality and allowing better access to the intracranial structures [1].

Of all tumor types, Glioblastoma Multiforme (GBM) and meningioma represent two of the

How to cite this article Florez E, Nichols TA, Lirette ST, Howard CM and Fatemi A. Developing a Texture Analysis Technique using Fluid-Attenuated Inversion Recovery (FLAIR) to Differentiate Tumor from Edema for Contouring Primary Intracranial Tumors. SM J Clin. Med. Imaging. 2018; 4(2): 1023.

most common primary intracranial tumors with a high incidence of clinical occurrence in adult patients [2,3]. It is known that the edema surrounding GBM contains both vasogenic and tumor cell infiltration, while the edema surrounding meningioma is a vasogenic type without tumor cell infiltration [4]. A comparison of images of vasogenic and infiltrative edema in patients with GBM, and vasogenic edema in patients with meningioma using Fluid-Attenuated Inversion Recovery (FLAIR) MRI images, may help to differentiate FLAIR signal changes between these two types of edema [5,6].

Once a brain tumor has been identified, there are several procedures for clinical treatment; the choice depends on the size and location of the tumor in the brain, the type of tissue involved, whether the tumor is benign or malignant, and its growth rate, among other factors [7,8]. Treatment options include surgery, chemotherapy and radiation therapy, or a combination of these. Surgical resection (if not deemed too dangerous) is usually the first treatment action to reduce pressure on the brain [9-13].

In recent years, new techniques have been developed for administering radiation to brain tumors while protecting nearby healthy tissues, avoiding and/or limiting the side effects that damage healthy tissues close to the tumor. Cells located in the region where treatment is received are injured or destroyed by radiation therapy, damaging their genetic material and slowing down their growth and constant division. It is not news that the effect of radiation damages both cancer cells and normal cells. However, many normal cells recover from the effects of radiation and regain proper function [13,14].

There are different techniques to identify the region where tumor cells are located within the brain. An emerging field of research achieving auspicious results is texture analysis. Texture analysis serves as a descriptor of pattern characteristics and identifier of various types of anatomical and pathological structures with applications in a wide variety of radiological topics across different medical imaging modalities including MRI [15-18].

Hypothetically, in MR imaging, the FLAIR signal of vasogenic/infiltrative edema differs uniquely in each patient with GBM. This study used T2W-FLAIR spin-echo MRI to differentiate between types of edema (vasogenic or tumor cell infiltrative) and extent of brain tumors in order to distinguish them through their textural properties. The results of this research may have potential applications, both as a staging procedure and a method of evaluating tumor response during treatment.

Materials and Methods

This study used a structure conformed by a set of consecutively interconnected stages: (a) selection of 3-D brain MRI patients diagnosed with intracranial tumor, (b) segmentation process of two regions of interest (ROI-1: edema and ROI-2: tumor), (c) extraction of texture features from the ROIs with different approaches (first-, second-, and higher-order statistics) and (d) statistical selection of the parameters providing the highest association for distinguishing tumors from edema. Figure 1 shows the sequence of modules used in this study.

Study population

Institutional Review Board (IRB) approval was obtained to access electronic medical records to identify and recruit thirty patients who underwent a brain MRI routine procedure from among hundreds of patients with similar clinical conditions. Of all patients, twenty patients had GBM (66 ± 8 years old, 12 females and 8 males) and ten patients had meningioma (64 ± 7 years old, 6 females and 4 males). All patients were selected by an experienced neuroradiologist with > 6 years of clinical experience. The inclusion criteria consisted of patients over 18 years of age who had an MRI between 2011 and 2016 with gliomas of various grades (based on WHO histological principles [19]), or a pre-operative MRI leading to a diagnosis of GBM or meningioma. Patients who received a pre-operative biopsy, corticosteroids at the time of the pre-operative MRI scan, and those with MRI images with severe artifacts, were excluded.

MR imaging acquisition

All thirty patients were scanned on a 3T scanner (SIEMENS, Skyra, USA) with a 16-channel RF head coil using T1-weighted contrast-enhanced fast-spoiled gradient-recalled acquisition with the following acquisition parameters: TR = 900 ms, TE = 8 ms, matrix size = 256 x 256, slice thickness = 4 mm, pixel bandwidth = 244.141 Hz. A T2-weighted FLAIR protocol was also used, with the following acquisition parameters: TR = 9002 ms, TE = 127.6 ms, TI = 880 ms, matrix size = 256 x 256, slice thickness = 5 mm, pixel bandwidth = 122.109 Hz. MRI scans were acquired prior to radiation treatment.

Image processing

Image processing represents the most demanding component of this study, since the relevant information used for analysis is extracted from the MR images. The main advantage of this mechanism is the use of non-invasive methods applied to the medical images assessed.

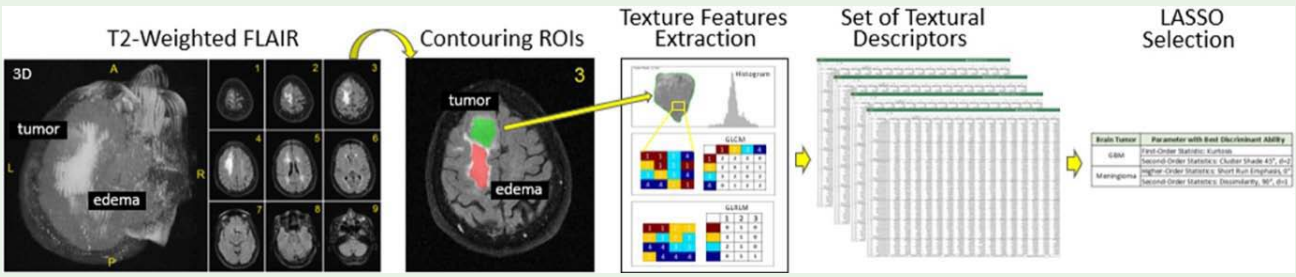

Figure 1: Flow chart with the sequence of modules used in this study: (a) T2W-FLAIR sequence of patients diagnosed with intracranial tumor, (b) contouring process of tumor and edema, (c) texture features extraction and, (d) statistical reduction and selection of the parameters with the best discriminant ability for distinguishing tumors from edema.

All image-processing steps were performed using in-house algorithms created in MatLab® version 2016a [20]. All images and data processing sequences used in this study allow the analysis of two-dimensional (2D) structures. Each sequence is detailed below.

Segmentation process: The segmentation process of medical images is considered one of the most complicated tasks in image processing. Segmentation allows subdividing an image or volume into regions or objects that compose it [18].

In this preliminary study the FLAIR signal of edema surrounding GBM, or meningioma was measured. The segmentation process was conducted manually by an experienced neuroradiologist with >6 years of clinical experience using a semiautomatic algorithm, identifying two regions of interest (ROI-1: edema and ROI-2: tumor) in all patients assessed as shown in Figure 2.

An expert neuroradiologist reviewed all FLAIR images and chose slices with generous and clear representation of the ROIs for segmentation. The choice of slices offered as much as information as possible from each region edema and tumor. The neuroradiologist used pre-determined colors to contour the tumor (green) and edema (red) regions in images for each member of the full cohort. Once manual contouring was completed, our algorithm generated a file with segmented regions; these files were used in the next step of the study.

Texture descriptors: Texture analysis is a technique widely used in several areas of modern medicine [17]. It uses the spatial variation of pixel intensities or patterns for different purposes including classification of different regions within the image, segmentation, characterization, and synthesis [16,18,21-24].

We have explored different texture analysis techniques focused primarily on statistical approaches with which about 300 diverse features of each segmented ROI (edema and tumor) were extracted. The texture features used in this study are distributed between three different techniques: first-, second- and higher-order statistics as explained below. All features formulas discussed herein are provided as supplementary information.

First-Order Statistics (FOS) represent the simplest way to calculate statistical features from the grey-level intensity histogram values of all pixels within an image, ranging from 0 to 2^ b-1, where b symbolizes the number of bits in the image (Figure 3a) [17]. This method measures standard descriptors to characterize the data. The histogram-based parameters calculated were mean, variance, SD, skewness, kurtosis, energy, entropy, contrast, coarseness and percentiles (1%, 10%, 50%, 90%, and 99%). However, the simplicity of this approach limits its robustness in discriminating unique textures in certain applications, as this method does not consider the spatial relationship, interaction and correlation of neighboring pixel values [25-27].

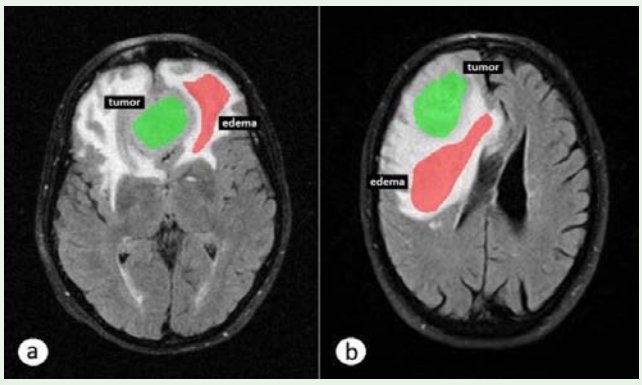

Figure 2: The segmentation process was conducted by an expert neuroradiologist through a semiautomatic algorithm, whereby two regions of interest (ROI-1: edema, red and ROI-2: tumor, green) were identified in patients diagnosed with (a) meningioma and (b) glioblastoma multiforme tumors.

Second-Order Statistics (SOS) describes the properties of pairs of pixel grey level values which occur in an ROI or image. This method uses the Grey Level Co-Occurrence Matrix (GLCM) which describes the relationships of pixel pairs considering different angles of orientation (θ = 0°, 45°, 90°, 135°) and separation between the reference and neighbor pixels [15,16,21]. The axes of GLCM are defined by the grey levels present in the image; these depend on the number of bits within the image (e.g. an 8-bit image will be displayed by 2^8 = 256 different grey levels). Based on the symmetry property, the GLCM transpose was calculated in order to include the results of the complementary orientations (θ = 180°, 225°, 270°, 315°) for its computation with the results of previously calculated orientations. Consequently, the symmetric matrix resulting from the sum of the regular and transposed GLCMs was used by convention. In brief, this technique allows the extraction of statistical information from an ROI or image from the distribution of pairs of pixels through the GLCM, as shown in Figure 3b [17,28,29].

Higher-order statistics (HOS) measure information on the run of a particular grey level of linearly adjacent pixels in particular directions for detecting non-linearities. A run is defined as a consecutive string of pixels with the same pixel intensity. Although HOS is an approach similar to SOS, certain applications have shown certain advantages of HOS mainly when analyzing images that present some kind of distortion due to effect of attenuation [30]. This method uses the Grey-Level Run Length Matrix (GLRLM) to represent information about the number of runs with pixels of defined grey-levels and run lengths in an image (Figure 3c). The number of pixels contained within the run is the run length [15,21,30-32]. For this study, we have incorporated the GLRLM for different run angles (θ = 0°, 45°, 90°, 135°).

Normalization Process: In image processing, it is quite common to apply normalization in order to modify the range of intensity values of the pixels which are part of the image or ROI being evaluated. Our study has provided calculation of the texture features through the different approaches indicated in the texture descriptors section from two perspectives: the first used ROIs without normalization (native images) and the other considered the same ROIs after a normalization process. A cumulative normalization method, 1% - 99%, was used in this study, a method often used in texture analysis [33,34]. This normalization process compresses the grayscale range of the image by considering the brightness level at which the cumulative histogram of image equals 1% of its total at the level where the cumulative histogram equals 99% of its total. The normalization processes are typically different for different images; different ROIs generally yield different 1%- 99% levels.

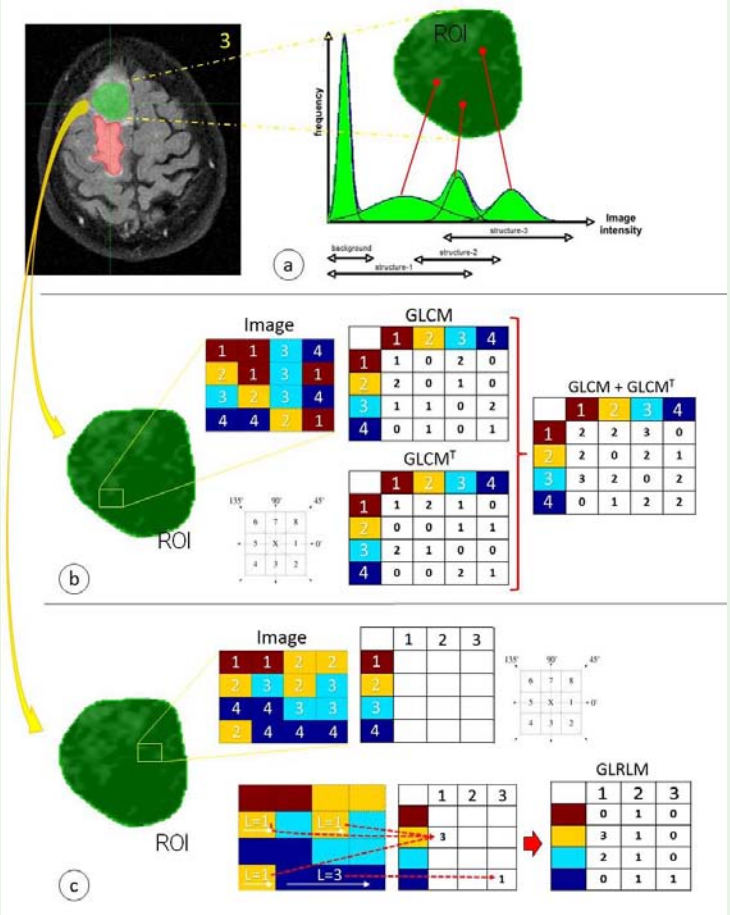

Figure 3: Texture analysis used in this study was distributed in different approaches: (a) First-order statistics based on the histogram distribution of the grey values, (b) Second-order statistics though the Gray-Level Co-Occurrence Matrix (GLCM), and (c) Higher-order statistics though the Gray-Level Run-Length Matrix (GLRLM).

Statistical analysis

As previously mentioned, all texture analysis methods applied in this study are statistical in nature. Those methods were computed for a population of specific ROIs and normalizations: edema and intracranial tumor, with- and without normalization. In this regard, the reduction and selection process were the result of a process of statistical estimation of a large database formed by all texture parameters antecedently calculated [35].

The least absolute selection and shrinkage operator (LASSO) is a variable selection method for linear regression models used in this study. The LASSO with binomial families and log it links was used to reduce and select the parameters that provide the highest association for distinguishing tumors from edema while shrinking irrelevant parameters. The LASSO performed a restriction process of all texture features through the absolute values of the parameters of the model. Those features whose regression coefficients are close to zero were eliminated. On the other hand, features with a strong association with the target variable of the corresponding model were selected. The selected features attempted to minimize the prediction error in the reduction and/or selection process to satisfy specific criteria of the process [36].

The standard operating procedure for feature selection in a texture analysis usually involves Principal Components Analysis (PCA) or Fisher scoring [37,38]. While both are valid methods for identifying clustering amongst parameters, they are agnostic to the target variable (edema versus tumor, in our case). Conversely, LASSO allows us to construct a model specifically tailored to classify tumor versus edema.

Finally, using the features selected from LASSO, the Receiver Operating Characteristic (ROC) analysis was performed and all relevant plots were constructed. The LASSO procedure was performed in R using the glmnet package; all other statistical procedures were performed using Stata v14.1 [39].

Results

Two-dimensional ROIs located in the edema and tumor was used for feature extraction for all patients with meningioma and GBM. After completing the sequence of processes described in the Materials and Methods section, a group of features selected through the LASSO procedure was obtained for patients with meningioma and GBM, both with- and without normalization. The selected parameters are listed in Table 1.

Table 1: Set of variables selected by LASSO procedure, including the feature with the best discriminant ability to differentiate edema from tumor tissue for different tumoral diseases and scenarios.

Brain Tumor	Type of Image	Variable with Best Discriminant Ability	All Variables selected by LASSO
Meningioma	Without normalization	First-Order Statistic 1% Percentile	First-Order Statistic: 1% Percentile
			Second-Order Statistics: Correlation, 90°, d = 4
			Second-Order Statistics: Correlation, 90°, d = 5
			Second-Order Statistics: Sum Average, 45°, d = 5
	With normalization	First-Order Statistic 1% Percentile	First-Order Statistic: 1% Percentile
			Second-Order Statistics: Correlation, 90°, d = 4
			Second-Order Statistics: Difference Variance, 90°, d = 4
Glioblastoma multiforme	Without normalization	Higher-Order Statistics Gray-Level Non-Uniformity, 90°	Higher-Order Statistic: Gray-Level Non-Uniformity, 90°
			First-Order Statistic: 1% Percentile
			Second-Order Statistics: Correlation, 0°, d = 3
			Second-Order Statistics: Correlation, 45°, d = 4
			Second-Order Statistics: Energy (ASM), 0°, d = 5
			First-Order Statistic: Skewness
			Second-Order Statistics: Sum Average, 45°, d = 5
	With normalization	Higher-Order Statistics Short Run Emphasis, 90°	Higher-Order Statistic: Short Run Emphasis, 90°
			First-Order Statistic: 1% Percentile
			Second-Order Statistics: Sum Entropy, 0°, d = 5
			Second-Order Statistics: Sum Entropy, 0°, d = 4
			Second-Order Statistics: Correlation, 90°, d = 4
			Second-Order Statistics: Sum Average, 45°, d = 3
			Area (cm²)

First-order statistics using 1% percentile feature was the only parameter chosen by LASSO in all four scenarios, and was the variable with the best discriminant ability for meningioma, with- and without normalization. Second-order statistics using correlation feature was also selected across scenarios, although the angle and the magnitude varied. For GBM, Higher-order statistics using gray level non-uniformity and short run emphasis features provided the best discrimination for images without and with normalization, respectively.

Although there was repetition of certain texture features in the different scenarios chosen as part of the LASSO selection process, these parameters do not have direct significance as the features with better discriminant capacity in all cases. In addition, other differentiated parameters with different distance values and/or angles were selected at the same time in some scenarios.

Figure 4 displays ROC results with both the single best discriminator (1% percentile for meningioma cases, gray-level non-uniformity 90° and short run emphasis 90° for GBM cases without normalization and with normalization, respectively) and the discriminant ability of the model using all parameters selected by LASSO. All univariate models had good discriminant ability (AUC>0.83), and all multivariate models had excellent discriminant ability (AUC>0.92).

Through the parameters with the best discriminant ability stratified by tissue that were listed in Table 1, the edema of the tumor tissue was clearly distinguished. Edema is represented by filled circles and intracranial tumor by open circles on FLAIR images for patients with meningioma and GBM. The dissociation between the two regions of interest (edema and tumor) is clear in all subjects and for all studied pathologies as shown in Figure 5.

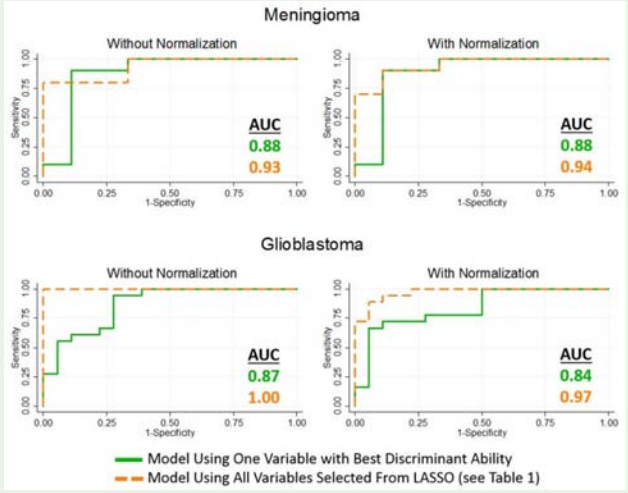

Figure 4: ROC curves showcasing both the single best discriminator (solid green lines) and the discriminant ability of the model using all variables selected by LASSO (dash orange lines).

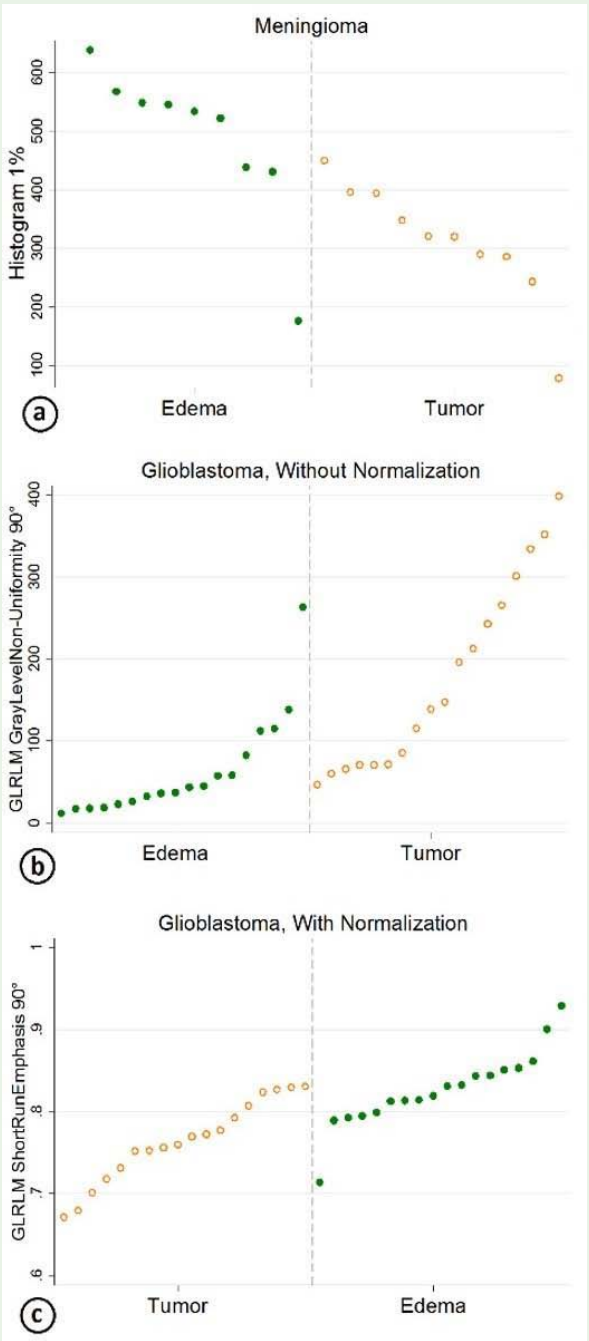

Figure 5: Sorted values for the best discriminator stratified by tissue: Edema (filled circles) and Brain tumor (open circles) on T2-FLAIR MR images for (a) Meningioma with and without normalization, (b) GBM without normalization and, (c) GBM with normalization.

Discussion

Brain tumors include a variety of complex particularities based on genetic-hereditary factors, radiation exposure, severe encephalocranial trauma, immunosuppression, hormonal factors, environmental factors (infections), and so on [1-3,6,7]. Despite its anatomopathological diversity, it is vital to have a reliable procedure to establish the histological diagnosis to increase the chances of treatment success.

Technological innovations are continuous and offer an important dimension in the treatment strategy for patients with brain tumors. Coadjuvant treatments are a radiation therapy shown to be effective in most malignant brain tumors, making their use unquestionable [7,8,11-14]; however, the success of this treatment depends directly on accuracy in estimating the size and location of the brain tumor [9-11].

In this scenario, texture analysis is capable of offering complementary information used by radiologists for the purposes of organization, diagnosis, and characterization of lesions or tumors within the brain. Texture analysis is widely applied in several areas of modern medicine considering different medical modalities, diverse organs and diseases [38]. We have used well-known concepts and different approaches (first-, second-, and higher-order statistics) for this purpose. In this study, extraction of the texture parameters was preceded by a semi-automatic and two-dimensional segmentation process of specific ROIs (edema and tumor). Future studies will improve some procedures, including the segmentation process, in order to extract much more information through the calculated texture parameters over 3D objects.

Based on a small number of texture parameters, the tumor regions in the brain were segregated, and the differentiation of the edema and the tumor tissue was established. In this study, the major innovation was the use of a different tool for the selection of the representative parameters that provide the highest association for distinguishing tumors from edema while shrinking irrelevant parameters. The most popular linear procedures used to reduce and select discriminant features are Principal Component Analysis (PCA) and Linear Discriminant Analysis (LDA) [40]; however, this study used a different selection operator, LASSO, which was applied to linear and nonlinear systems with encouraging results. Different procedures for the reduction and selection of discriminant parameters (i.e. PCA, LDA, LASSO, and so on) have attendant advantages and disadvantages. Nowadays, many disadvantages of the procedures for reduction and selection of parameters can be overcome by using hybrid models (i.e. PCA+LASSO) as they generate better selection processes.

In clinical terms, GBM is generally considered a solitary tumor (commonly located in both frontal lobes) while meningioma is not [41]. Of course, this is not a univocal rule; however, each type of tumor has a distinctive biologic nature. On this basis, our results suggest morphological differentiation between the two different brain pathologies evaluated (meningioma and GBM), taking into consideration different ROI locations, sizes, and shapes.

In addition, we can take advantage of multiparametric quantitative MRI imaging for better tumor and edema classification. These methods including, for instance, diffusion tensor imaging (DTI) and all of its quantitative derivatives, such as Fractional Anisotropy (FA), Medium Diffusivity (MD), Linear Coefficient (CL), Flat Coefficient (CP) and Spherical Coefficient (CS) imaging [42]. Some encouraging results have also been reported from the combination of Arterial Spin Labeling (ASL) perfusion and Diffusion Tensor Imaging (DTI) metrics of the enhanced lesion and related edema in the process of identifying recurrent/residual gliomas [43].

Conclusion and Future Work

According to the values of the descriptors selected by LASSO (Table 1) and based on their theoretical definitions, this study showed that meningioma images generally exhibit more similarity and linear dependence between the intensity values of their elements than images of GBM. That statement should be taken with caution since it only refers to the cases analyzed in this study and cannot be taken as a general condition. Further studies need to be performed with a greater number of subjects to examine this relationship. In addition, the analysis of more patients will allow having a much clearer position regarding the levels of infiltration in tumors such as meningioma and GBM.

Our FLAIR-based method has potential to be used as a beneficial and noninvasive alternative for differentiation and/or classification of these tumor types through specific descriptors. Small subsets of texture descriptors show excellent ability to discriminate edema from tumor tissue.

Future studies will evaluate different MRI sequences such as diffusion-weighted and ADC images with some transformations techniques applied to input images. In addition, texture exploration could be improved by extending that technique from 2-D to 3-D analysis.

Acknowledgments

The preparation of this original article was supported by the Department of Radiology at The University of Mississippi Medical Center - Jackson, MS.

References

1. Claussen C, Fahlbusch R, Felix R, Grumme T, Heinzerling J, Kazner, E et al. Computed Tomography and Magnetic Resonance Tomography of Intracranial Tumors. A Clinical Perspective. Springer-Verlag Berlin Heidelberg. 1988.
2. DeAngelis LM, Gutin PH, Leibel SA, Posner JB. Intracranial Tumors: Diagnosis and Treatment. Martin Dunitz Ltd, a member of the Taylor & Francis e-Library. 2002.
3. Mehndiratta A, Tee YK, Payne SJ, Chappell MA. Tumors of the Central Nervous System: Pineal, Pituitary, and Spinal Tumors (Volume 11). Springer Science+Business Media Dordrecht. 2014.
4. Bradac GB, Bull U, Fahlbusch R, Fahlbusch R, Grumme T, Kazner E, et al. Computed Tomography in Intracranial Tumors. Springer-Verlag Berlin Heidelberg. 1982.
5. Taphoorn MJB, Heimans JJ, Kaiser MC, de Slegte RG, Crezee FC, Valk J. Imaging of brain metastases. Neuroradiology.1989; 31: 391-395.
6. Bodey B, Siegel SE, Kaiser HE. Molecular Markers of Brain Tumor Cells Implications for Diagnosis, Prognosis and Anti-Neoplastic Biological Therapy. Springer Science + Business Media, Inc. 2005.
7. Bähr O, Steinbach JP, Weller M. Brain tumor imaging. Medical Radiology Radiation Oncology. Springer 2016.
8. Ali-Osman F. Brain tumors. Contemporary Cancer Research. Humana Press Inc. 2005.
9. Baehring JM, Piepmeier JM. Brain Tumors: Practical Guide to Diagnosis and Treatment. Neurological Disease and Therapy. CRC Press. 2006.
10. Thapar K, Rutka JT, Laws ER. Brain edema, increased intracranial pressure, vascular effects, and other epiphenomena of human brain tumors. In: Kaye AH, Laws ER, eds. Brain tumors. New York: Churchill Livingstone.1995; 163-189.
11. Meyer JL, Kavanagh BD, Purdy JA, Timmerman R. IMRT, IGRT, SBRT - Advances in the Treatment Planning and Delivery of Radiotherapy. Frontiers of Radiation Therapy and Oncology. 2007; 40.
12. Newton HB. Handbook of Neuro-Oncology Neuroimaging. Academic Press. Elsevier Ltda. 2007.
13. Jellinger K, Voth D, Mundinger F, et al. Therapy of Malignant Brain Tumors. Springer-Verlag/Wien, 1987.
14. Graham CA, Cloughesy TF. Brain tumor treatment: Chemotherapy and other new developments. Seminars in Oncology Nursing. 2004; 20: 260-272.
15. Haralick RM, Shanmugam K, Dinstein I. Textural Features of Image Classification, IEEE Transactions on Systems, Man and Cybernetics.1973; 6.
16. Kassner RE, Thornhill RE. Texture Analysis: A Review of Neurologic MR Imaging Applications. AJNR Am J Neuroradiol. 2010; 31: 809-816.
17. Galleno G, Bonilha L, Li LM, Cendes F. Texture analysis of medical images. Clin Radiol. 2004; 59:1061-1069.
18. Rangayyan RM. Texture in Biomedical Images. Analysis of Texture. CRC Press. 2004.
19. Louis DN, Perry A, Reifenberger G, Von Deimling A, Figarella-Branger D, Cavenee WK, et al. The 2016 World Health Organization Classification of Tumors of the Central Nervous System: a summary. Acta Neuropathol. 2016; 131:803-820.
20. MATLAB® and Statistics Toolbox Release 2016a. Natick, Massachusetts: The MathWorks Inc.
21. Nailon WH. Texture Analysis Methods for Medical Image Characterisation. Biomedical Imaging, Youxin Mao. InTech. 2010.
22. Mirmehdi M, Xie X, Suri J. Texture Modelling and Synthesis and, A Galaxy of Texture Features. Handbook of Texture Analysis. Imperial College Press. 2008.
23. Bharati MH, Liu JJ, MacGregor JF. Image texture analysis: methods and comparisons. Chemometrics and Intelligent Laboratory Systems. 2004; 72:57-71.
24. Parmar C, Rios Velazquez E, Leijenaar R, Jermoumi M, Carvalho S, Mak RH et al. Robust Radiomics Feature Quantification Using Semiautomatic Volumetric Segmentation. PLoS ONE. 2014; 9: e102107.
25. Hassan A, Ahmed S, Gar-elnabi M, Ali Omer MA, Ahmed A. Characterization of Hepatocellular Carcinoma (HCC) in CT Images using Texture Analysis Technique. International Journal of Science and Research (IJSR). 2016; 5.
26. Tuceryan M. Texture Analysis. The Handbook of Pattern Recognition and Computer Vision. World Scientific Publishing Co.1998; 207-248.
27. Amadasun M, King R. Textural Features Corresponding to Textural Properties. IEEE Transactions on Systems, Man, and Cybernetics. 1989; 19: 1264 - 1274.
28. Soh L, Tsatsoulis C. Texture Analysis of SAR Sea Ice Imagery Using Gray Level Co-Occurrence Matrices. IEEE Transactions on Geoscience and Remote Sensing. 1999; 37: 780 - 795.
29. Iausi DA. An analysis of co-occurrence texture statistics as a function of grey level quantization, Can. J. Remote Sensing. 2002; 28: 45-62.
30. Galloway M. Texture Analysis using Gray Level Run Lengths. Computer Graphics and Image Processing. 1975; 4: 172-179.
31. Chu A, Sehgal CM, Greenleaf JF. Use of gray value distribution of run lengths for texture analysis. Pattern Recognition Letters.1990; 11: 415-419.
32. Dasarathy BV, Holder EB. Image characterization based on joint gray level-run length distribution. Pattern Recognition Letters. 1991; 12: 497-502.
33. Materka A. Texture analysis methodologies for magnetic resonance imaging. Dialogues ClinNeurosci. 2004; 6: 243, 2004.

34. Nuyl LG, Udupa K. On standardizing the MR image intensity scale. Magn Reson Med. 1999;42:1072-1081.

35. Benoit-Cattin H, Bezy-Wendling J, Collewet G. Statistical methods. Texture Analysis for Magnetic Resonance Imaging. European Network Cost Action B21, Med4publishing s.r.o. 2006.

36. Tibshirani R. Regression shrinkage and selection via the lasso. J. Royal. Statist. Soc B. 1996; 58: 267-288.

37. Wise B, Ricker N, Veltkamp DF, Kowalski BR. A theoretical basis for the use of principal components model for monitoring multivariate processes. Proc. Control Qual.1990; 1:41-51.

38. Depeursinge A, Foncubierta-Rodriguez A, Van de Ville D, Müller H. Three-dimensional solid texture analysis in biomedical imaging: Review and Opportunities. Medical Image Analysis. 2014; 18: 176-196.

39. StataCorp. Stata Statistical Software: Release 14. College Station, TX: StataCorp LP. 2015.

40. Witjes H, Rijpkema M, van der Graaf M, Melssen W, Heerschap A, Buydens L. Multispectral Magnetic Resonance Image Analysis Using Principal Component and Linear Discriminant Analysis. J Magn Reson Imaging. 2003; 17: 261-269.

41. Larjavaara S, Mantyla R, T Salminen, Haapasalo H, Raitanen J, Jääskeläinen J, et al. Incidence of gliomas by anatomic location. Neuro Oncol. 2007; 9: 319-325.

42. El-Serougy L, Abdel Razek AA, Ezzat A, Eldawoody H, El-Morsy A. Assessment of diffusion tensor imaging metrics in differentiating low-grade from high-grade gliomas. Neuroradiol J. 2016; 29: 400-407.

43. Razek AAKA, El-Serougy L, Abdelsalam M, Gaballa G, Talaat M. Differentiation of residual/recurrent gliomas from postradiation necrosis with arterial spin labeling and diffusion tensor magnetic resonance imaging-derived metrics. Neuroradiology. 2018; 60: 169-177.